China Ocean Eng., Vol. 26, No. 1, pp. 37 – 48

DOI 10.1007/s13344-012-0003-7, ISSN 0890-5487

Numerical Investigation of the Effect of Current on Wave Focusing*

LI Jin-xuan (李金宣)[a, b, 1], LIU Dian-yong (刘殿勇)[a] and LIU Shu-xue (柳淑学)[a]

[a] *Key State Laboratory of Coastal and Offshore Engineering*, *Dalian University of Technology*, *Dalian 116023*, *China*

[b] *Key Laboratory of Coastal Disasters and Defence of Ministry of Education*, *Hohai University*, *Nanjing 210098*, *China*

(Received 5 May 2011; received revised form 28 August 2011; accepted 16 October 2011)

ABSTRACT

In the present study, a numerical wave tank is developed to simulate the nonlinear wave-current interactions based on High Order Spectral (HOS) method. The influences of current on wave focusing are investigated by use of numerical model. The current is assumed to be constant in space. Focused waves with different amplitudes and frequency spectra are simulated with and without current. The focused wave characteristics, such as surface elevation, the maximum crest and frequency spectrum, with different current are compared. The results show that the opposing current increases the maximum crest and the energy transform during wave focusing process, and vice versa for the following current.

Key words: *wave-current interaction*; *high order spectral method*; *numerical wave tank*

1. Introduction

Freak waves, also called rouge waves, impose large or extreme forces on ship and offshore structures. It can cause severe damage to offshore structures and endanger human lives. As a result of climate change, the risk of having more severe events is likely to increase. In the last 20 years, many researchers have paid attention to the mechanisms of freak wave generation. Several mechanisms were used to explain freak wave generation, such as wave focusing, wave-current interaction and modulation instability (Kharif and Pelinovsky, 2003). Among these mechanisms, wave focusing is the most important mechanism and was studied by many researchers, such as Rapp and Melville (1990), Baldock and Swan (1996), Johannessen and Swan (2003), Gibson and Swan (2007), and Fochesato *et al*. (2007). Most of these studies were conducted on quiescent water. However, there are current existences in the real ocean. The freak waves are observed frequently in the region of the world ocean with strong currents. The influences of current on wave focusing can not be neglected. Unfortunately, wave-current interaction received less attention for the generation of focused waves. Only recently, freak wave generation on current was investigated by Wu and Yao (2004), Touboul *et al*. (2007), and Lavrenov and Porubov (2006). Wu and Yao (2004) experimentally studied the limiting freak wave in currents. Touboul *et al*. (2007) numerically studied the nonlinear focused wave group on current. Lavrenov and

* This research was partially supported by the Specialized Research Fund for the Doctoral Program of Higher Education of China (Grant No. 20090041120023) and Open Research Fund Program of Key Laboratory of Coastal Disasters and Defence of Ministry of Education of China, and the National Natural Science Foundation of China (Grant No. 50921001).
1 Corresponding author. E-mail: lijx@dlut.edu.cn

Porubov (2006) investigated three reasons for freak wave generation due to wave interaction with non-uniform current.

In order to better understand the freak wave properties, the influence of current on wave focusing is numerically investigated based on High Order Spectral method in the present study. The model and its verification will be introduced in Section 2. Then the surface elevation, the maximum crest and the frequency spectrum of focused wave with and without current are given in Section 3. Lastly, the conclusions are summarized in Section 4.

2. Numerical Model

2.1 Governing Equations

It is assumed that the fluid is irrotational and inviscid. A Cartesian coordinate system is employed such that the $z = 0$ corresponds to the still water level and z is positive upwards. For 2D surface wave propagation problem with a steady uniform current parallel to x-direction, the total velocity potential Φ in the fluid domain can be expressed as $\Phi = U_0 x + \phi$, where U_0 denotes the uniform current and ϕ is the wave velocity potential. The potential satisfies the Laplace equation:

$$\nabla^2 \Phi(x,z,t) = \nabla^2 \phi(x,z,t) = 0 \,. \tag{1}$$

The fully nonlinear free surface boundary conditions expressed by the velocity potential on the water surface can be written as:

$$\frac{\partial \eta}{\partial t} = \frac{\partial \Phi}{\partial z} - \nabla_x \Phi \, \nabla_x \eta \,, \quad z = \eta; \tag{2}$$

$$\frac{\partial \Phi}{\partial t} = -\mathrm{g}\eta - \frac{1}{2}\left|\nabla_x \Phi\right|^2 + \frac{1}{2}\left(\frac{\partial \Phi}{\partial z}\right)^2 - \frac{P_\mathrm{a}}{\rho}, \quad z = \eta, \tag{3}$$

where P_a is the atmospheric pressure, and $\nabla_x = \partial/\partial x$. Substituting $\Phi = U_0 x + \phi$ into Eqs. (2) and (3) yields the free surface boundary conditions as follows:

$$\frac{\partial \eta}{\partial t} = \frac{\partial \phi}{\partial z} - \nabla_x \phi \, \nabla_x \eta - U_0 \nabla_x \eta \,, \quad z = \eta; \tag{4}$$

$$\frac{\partial \phi}{\partial t} = -\mathrm{g}\eta - \frac{1}{2}\left|\nabla_x \phi\right|^2 + \frac{1}{2}\left(\frac{\partial \phi}{\partial z}\right)^2 - U_0 \nabla_x \phi - \frac{P_\mathrm{a}}{\rho}, \quad z = \eta. \tag{5}$$

Generally, lateral boundaries of the computation domain are either fixed or moving boundaries. For the wave tank, the incident wave is generated by a wave maker with motion $X(t)$ at the left boundary. So the linear boundary condition can be written as:

$$\frac{\partial \Phi}{\partial x} = \frac{\partial \phi}{\partial x} + U_0 = \frac{\partial X}{\partial t} + U_0 \quad \text{or} \quad \frac{\partial \phi}{\partial x} = \frac{\partial X}{\partial t} \quad \text{on} \quad x = 0. \tag{6}$$

For the wave velocity potential ϕ, the boundary condition on the right side of the computation domain is no-flux condition. It can be written as:

$$\frac{\partial \Phi}{\partial x} = \frac{\partial \phi}{\partial x} + U_0 = U_0 \quad \text{or} \quad \frac{\partial \phi}{\partial x} = 0 \quad \text{on} \quad x = L_x. \tag{7}$$

The condition on bottom can be written as:

$$\frac{\partial \Phi}{\partial z}=\frac{\partial \phi}{\partial z}=0 \quad \text{on} \quad z=-h. \tag{8}$$

2.2 Numerical Procedure

In the present study, the governing equations are solved by High Order Spectral (HOS) method proposed by Dommermuth and Yue (1987). As in Zakharov (1968), the free surface boundary conditions (4) and (5) can be rewritten as:

$$\frac{\partial \eta}{\partial t}=\left(1+\left|\nabla_x \eta\right|\right)\frac{\partial \phi}{\partial z}-\nabla_x \phi^s \nabla_x \eta-U_0 \nabla_x \eta \quad \text{on} \quad z=\eta \tag{9}$$

$$\frac{\partial \phi^s}{\partial t}=-g\eta-\frac{1}{2}\left|\nabla_x \phi^s\right|^2+\frac{1}{2}\left(1+\left|\nabla_x \eta\right|^2\right)\left(\frac{\partial \phi}{\partial z}\right)^2-U_0 \nabla_x \phi^s-\frac{P_a}{\rho} \quad \text{on } z=\eta \tag{10}$$

where $\phi^s(x,t)=\phi(x,\eta,t)$ is the velocity potential on the water surface.

In order to solve this non-homogeneous boundary condition, following Bonnefoy *et al.* (2004), the velocity potential ϕ^s can be split into the sum of a prescribed non-periodic components and an unknown period component, i.e., $\phi^s=\phi_f^s+\phi_w$. Substituting this equation into Eqs. (9) and (10), and setting P_a to be zero, the free surface boundary conditions can be written as:

$$\frac{\partial \eta}{\partial t}=[1+(\nabla_x \eta)^2]\frac{\partial \phi_f^s}{\partial z}-\nabla_x \phi_f^s \nabla_x \eta+\frac{\partial \phi_w}{\partial z}-\nabla_x \phi_w \nabla_x \eta-U_0 \nabla_x \eta \qquad z=\eta; \tag{11}$$

$$\begin{aligned}\frac{\partial \phi_f^s}{\partial t}=&-\frac{\partial \phi_w}{\partial t}-g\eta-\frac{1}{2}\left|\nabla_x \phi_f^s\right|^2+\frac{1}{2}[1+(\nabla_x \eta)^2]\left(\frac{\partial \phi_f}{\partial z}\right)^2-\nabla_x \phi_f^s \nabla_x \phi_w\\&-\frac{1}{2}\left(\frac{\partial \phi_w}{\partial z}\right)^2-\frac{1}{2}\left|\nabla_x \phi_w\right|^2-U_0(\nabla_x \phi_f^s+\nabla_x \phi_w), \qquad z=\eta,\end{aligned} \tag{12}$$

where the prescribed non-periodic component ϕ_w satisfies the wave maker boundary condition (6) and other lateral boundary conditions (7). It can be chosen as different expansions, and a spectral expansion is employed in this paper referred to Bonnefoy *et al*. (2004) and Li *et al*. (2008). The unknown period component ϕ_f satisfies the free surface Eqs. (11) and (12) and the lateral boundary condition Eq. (7). It can be solved by HOS method proposed by Dommermuth and Yue (1987).

Besides, the initial condition for this problem is

$$\begin{cases}\eta(x,\, t=0)=0\\ \Phi(x,\, t=0)=U_0 x\end{cases} \tag{13}$$

For a wave maker boundary, the velocity potential ϕ_w should be pre-solved by Eq. (6) before the time integration is conducted. According to linear wave maker theory, the incident velocity can be calculated by the following equation for a specified wave, i.e.

$$\frac{\partial X}{\partial t}=\frac{\omega_r}{T(k_0)}\eta, \tag{14}$$

where η is the expected water waves. ω_r is the circular wave frequency satisfying the following

equation:

$$\omega_r^2 = (\omega - kU_0)^2 = kg\tanh(kh)\,, \tag{15}$$

$T(k_0)$ is the transfer function for piston type wave maker and can be calculated by the following equation for two-dimensional waves.

$$T(k_0) = \frac{2[\cosh(2k_0h) - 1]}{2k_0h + \sinh(2k_0h)}\,, \tag{16}$$

where k_0 is the wave number on still water.

2.3 Verification of the Numerical Model

For the investigation of the accuracy of this model, regular wave-current interactions in the deep water and intermediate water are calculated. The used parameters are shown in Table 1. The deep water cases (A1 to A3) are used to examine the accuracy of the present numerical model and the intermediate water cases (B1 to B3) are used to investigate the effect of nonlinear interaction between wave and current. Fig. 1 gives the comparison between the calculated water surface elevations by the present numerical method (solid line) and analytical solution (dot) for cases A1 to A3 at location x = 15.0 m. It shows that the calculated results agree well with the analytic results. It also can be seen that the wave amplitude with following current is smaller than the input wave amplitude, and the wave amplitude with opposing current is bigger than the input amplitude. Fig. 2 shows the calculated results for cases B1 to B3 at location x = 15.0 m. These results are compared with that of multi-layer Boussinesq-type model (Lynett, 2002). The comparison is excellent and confirms that the accuracy of the present numerical model is satisfactory. The results show that the wave amplitude of following current case is bigger than the input wave amplitude, though following current reduces wave amplitude. This contributes to the effect of nonlinear interaction of wave-wave and wave-current and the nonlinear wave transformation because of shallow water. In addition, it is shown that the wave crests become higher and sharper, wave troughs become shallower and flatter during wave propagation because of nonlinear interaction, especially for the case of wave with opposing current.

Table 1 Input parameter of cases

Case	A (m)	T (s)	L (m)	H (m)	U_0 (m/s)	h/L
A1	0.025	1.0	1.56	1.0	0.1	1/1.56
A2	0.025	1.0	1.56	1.0	0	1/1.56
A3	0.025	1.0	1.56	1.0	–0.1	1/1.56
B1	0.1	4.17	12.55	1.0	0.313	1/12.55
B2	0.1	4.17	12.55	1.0	0	1/12.55
B3	0.1	4.17	12.55	1.0	–0.313	1/12.55

A: wave amplitude; T: wave period; L: wave length; h: water depth.

Fig. 1. Comparison of the wave elevation calculated by the present numerical model (solid lines) with linear analytic (dots) theory at location x = 15.0 m for deep water cases A1~A3.

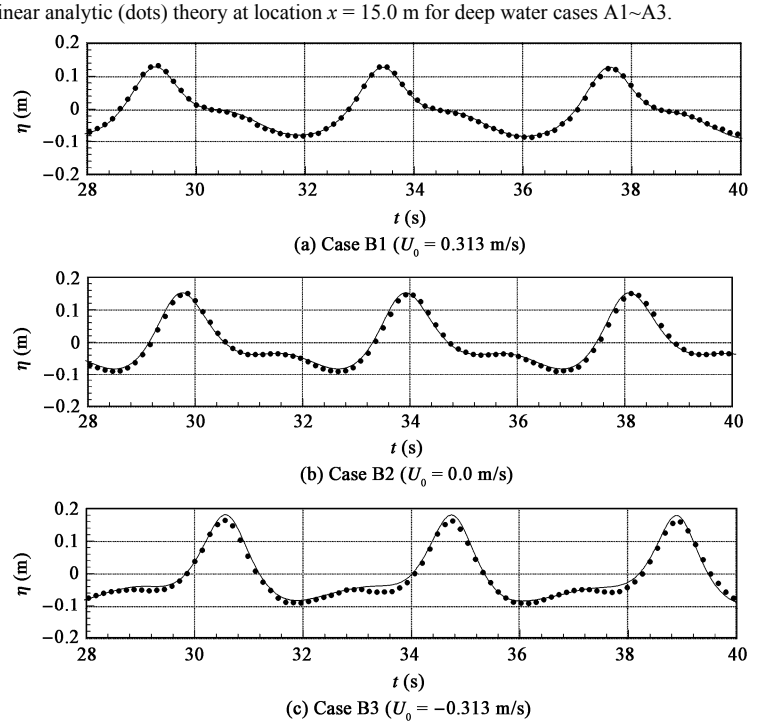

Fig. 2. Comparison of the calculated wave elevation by the present numerical model (solid lines) with multi-layer Boussinesq model (dots) at location x=15.0 m for shallow water cases B1~B3.

3. Numerical Study on Wave Focusing with Current

3.1 Focused Wave Generation with Current

The wave focusing method is usually used to generate extreme or breaking waves (Rapp and Melville, 1990; Nepf *et al*., 1998; Liu and Hong, 2005). In this study, the interaction between wave and current is considered. The focused wave generation on current can be described as follows.

According to linear theory, the free water surface $\eta(x, t)$ can be calculated by

$$\eta(x,t)=\sum_{i=1}^{N_f} a_i \cos(k_i x-\omega_{ri} t-\varphi_i)\,, \tag{17}$$

where N_f is the number of frequency; a_i is the component wave amplitude with the i-th frequency ω_{ri}, k_i is the wave number and φ_i the phase of wave component. Frequency ω_{ri} and the wave number k_i are related to each other by the linear dispersion equation (15). If the waves are assumed to be focused at the specified position x_b and time t_b, then φ_i can be calculated by

$$\varphi_i = k_i x-\omega_{ri} t+2m\pi \quad m=0,\ \pm 1,\ \pm 2,\cdots \tag{18}$$

By substituting Eq. (18) into Eq. (17), the wave surface that is focused at position x_b and time t_b can be written as:

$$\eta(x,t)=\sum_{i=1}^{N_f} a_i \cos[k_i(x-x_b)-\omega_{ri}(t-t_b)]\,. \tag{19}$$

The wave amplitude of each wave component can be determined according to the assumed wave spectrum. In the present study, two different wave spectra are used to examine the effect of wave spectrum on focused wave characteristics. The first is called the constant-wave-amplitude (CWA) distribution, i.e. a spectrum with a "top hat" shape. This means that the amplitude of each component wave a_i is constant. So a_i can be derived as:

$$a_i=\frac{A}{N_{\mathrm{f}}}\,, \tag{20}$$

where A is the assumed focused wave amplitude. The second kind of frequency spectrum is called the constant-wave-steepness (CWS) distribution and is a spectrum with a sharp peak. In this case, the component wave steepness is assumed to be constant, i.e., $k_i a_i$ = const. Also, we assume $A=\sum_{i=1}^{N_f} a_i$. Then a_i can be determined according to the given focused wave amplitude A by the following equation:

$$a_i=\frac{A}{k_i\sum_{i=1}^{N_f}\frac{1}{k_i}}\,. \tag{21}$$

In addition, the discrete frequency f_i is uniformly spaced over the frequency band $[f_1, f_n]$. The frequency width Δf and the central frequency f_c are defined as:

$$\Delta f=f_n-f_1 \quad \text{and} \quad f_{\mathrm{c}}=(f_1+f_n)/2\,. \tag{22}$$

3.2 Numerical Results

In this section, the characteristics of the focused wave with and without current are investigated

by the developed HOS model. Table 2 lists the parameters used in the study. Varied focusing amplitudes are used and current is varying from –0.3 m/s to 0.3 m/s. In addition, two different wave spectra are used, and the central frequency and frequency band is chosen as 0.83 Hz and 0.56 Hz, respectively.

Table 2 Input parameter of focused wave cases

Case	f_c (Hz)	f (Hz)	U_0 (m/s)	A (m)	Spectrum	h (m)
1	0.83	0.55~1.11	–0.3~0.3	0.01~0.06	CWA	3.0
2	0.83	0.55~1.11	–0.3~0.3	0.01~0.06	CWS	3.0

3.2.1 *Surface Elevations*

Fig. 3 compares the surface displacement elevation of the focused wave at different locations on different currents: U_0 = –0.1 m/s, 0.0 m/s and 0.1 m/s. In this plot, x^* is the distance relative to the theoretical focusing point, $x^* = x – x_b$. As expected, it can be seen that the short waves are ahead of the long waves and the surface elevation becomes steeper and steeper when the wave packets are approaching the assumed focusing point. After passing the focusing location, they disperse gradually and so the longer waves go ahead of the shorter waves. By comparing the surface elevations with different currents, it is shown that the surface elevation with opposing current leads ahead of the waves with zero and following current at upstream locations, and this phenomenon is reversed at downstream locations.

3.2.2 *Surface Elevations at Focusing Point*

Fig. 4 shows the surface elevation of the focused wave on U_0 = 0.1 m/s, 0.0 m/s, and –0.1 m/s at the focusing point. Here, the focusing point is defined as the location where the maximum crest of the focused wave group occurred. Owing to the nonlinear interaction, the actual focusing point is usually shifted downstream. For these cases, the focusing point located between x^* = 0.0 m and x^* = 1 m. The figure shows that the focused surface profile for the opposing current becomes steeper, and vice versa for following current. It means that there are stronger nonlinear interactions during the wave focusing process with opposing current. There are the same results for CWA and CWS spectrum.

3.2.3 *Maximum Crests*

Fig. 5 gives the numerically calculated maximum crests for different currents. The maximum crest is normalized by the input amplitude in the figure. This figure shows that as expected, owing to the nonlinear interaction of wave-wave and wave-current, the maximum crest for opposing currents cases increases with the increasing current velocity and that for following current cases decreases with the increasing current velocity. There are similar phenomena for focused waves with CWA and CWS spectrum, but the maximum crests for CWA cases are bigger than that for CWS cases.

The wave amplitude of focused waves can also affect the maximum crest. This is clearly shown in Fig. 6. For opposing current cases and zero current cases, the maximum crest of focused wave groups is bigger than the input assumed focused amplitude and the rate of the maximum crest and the input amplitude increases with the increasing amplitude. For opposing current, when the amplitude is small

(weak nonlinear cases), the maximum crest of following current cases is smaller than the input assumed focused amplitude. But when the amplitude is large (strong nonlinear cases), the maximum crest with following current can be bigger than the input assumed focused wave amplitude, even though the following current decreases wave amplitude.

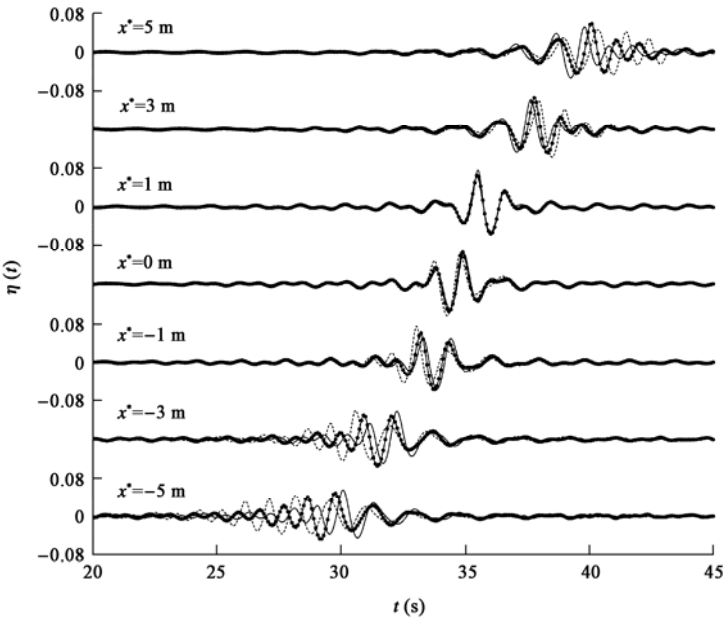

Fig. 3. Surface elevation of focused waves on current: U_0 = 0.1 m/s (solid lines), 0.0 m/s (solid line with circles), and −0.1 m/s (dashed lines) at different locations (A = 0.06 m, CWA, h = 3.0 m).

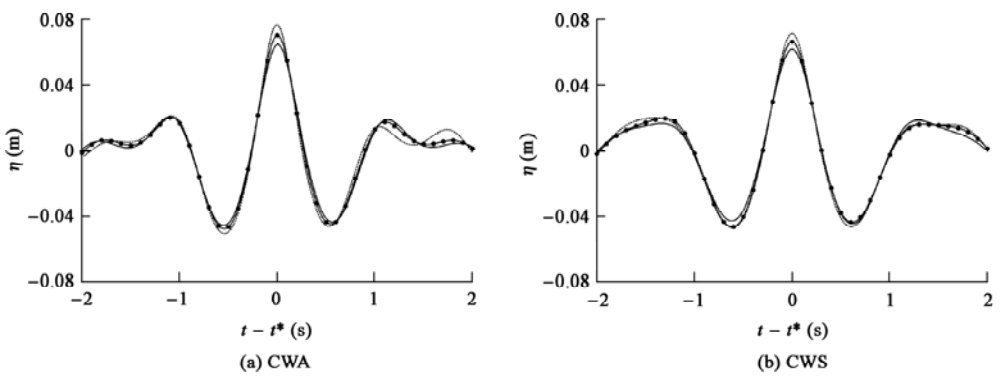

Fig. 4. Surface elevation of focused waves on current: U_0 = 0.1 m/s (solid lines), 0.0 m/s (solid line with circles) and −0.1 m/s (dashed lines) at focusing point (A = 0.06 m, h = 3.0 m).

3.2.4 *Frequency Spectra of the Focusing Waves*

Figs. 7~9 show the variation of the amplitude spectra of the surface elevation during the focusing process of the focused wave with and without current. In the figures, the amplitude spectrum is normalized by the central frequency f_c and central wave number k_c. The wave spectra at five

representative positions (including four fixed positions and the accurate focusing point for each case) are given to show the variation of the amplitude wave spectra during the wave transformation and the dashed lines and solid lines represent the amplitude spectrum at the upstream reference position (x^*=–6.0 m) and at the marked positions, respectively. Fig. 7 shows the amplitude spectra of surface elevations of the focused wave without current. As many earlier studies (Rapp and Melville, 1900; Liu *et al.*, 2008), there are no significant changes within input frequency band (0.55~1.15 Hz), but there are a few differences within higher frequency. These differences become most obvious at focusing point (x^*=0.55 m for CWA and x^*=0.35 m for CWS). It means that there is energy transfer between the wave components due to the wave-wave interactions during the wave transformation. This energy transfer to higher frequency for CWA spectra cases is bigger than that for CWS spectra cases. It means that energy distributions can influence the energy transfer during the wave focusing process.

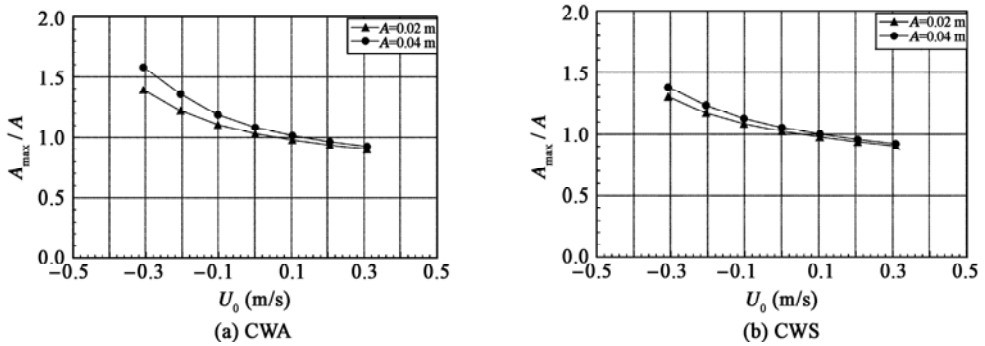

Fig. 5. Variation of the maximum focused wave crest with current velocity.

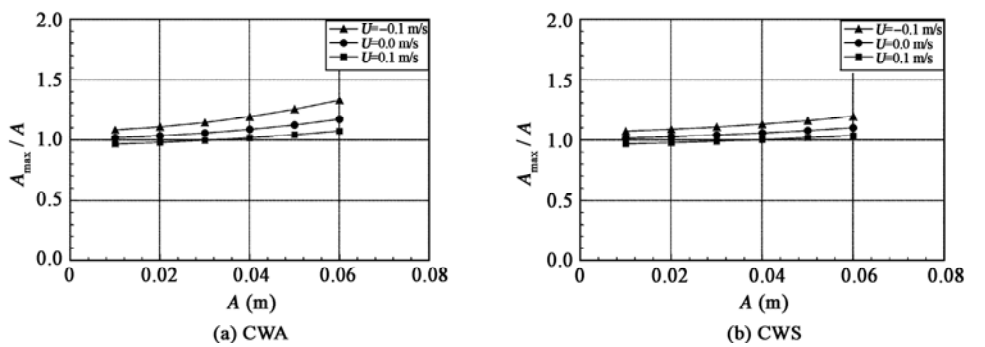

Fig. 6. The variation of the maximum focused wave crest with the input focusing amplitude.

Fig. 8 and Fig. 9 give the variation of the amplitude spectra of the surface elevations of the focused wave with following and opposing current, respectively. Though similar phenomena of energy transfer to higher frequency can be observed, there is a difference between following and opposing current cases. The energy transfer of the focused wave with opposing current is more significant than that with following current. It means that the focused wave with opposing current has stronger nonlinearity. This is identical to the phenomena shown by the focusing wave surface as previously discussed.

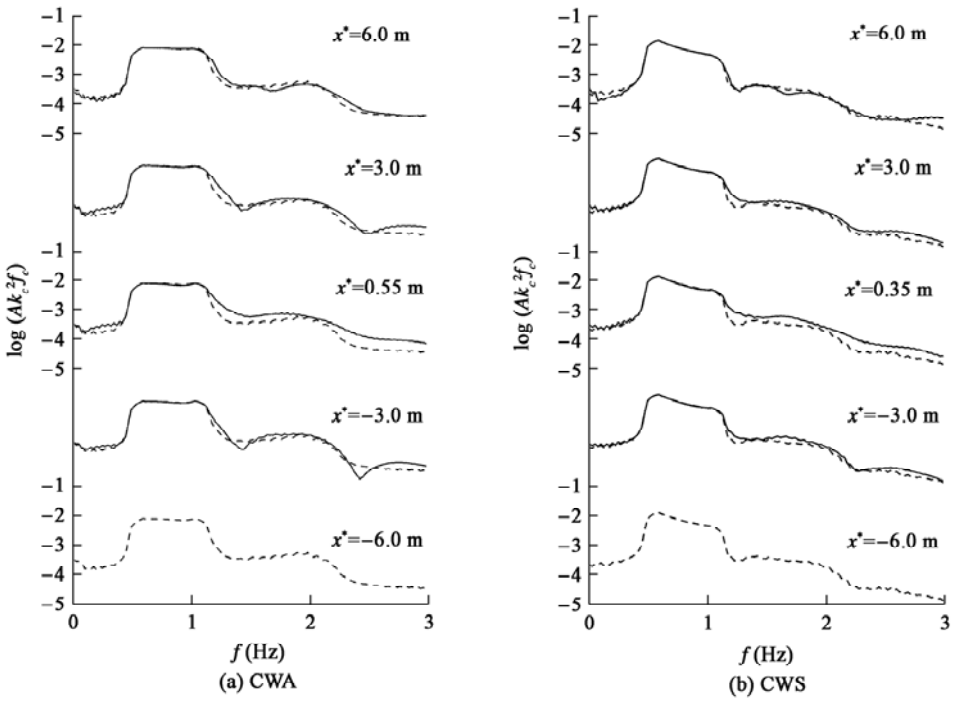

Fig. 7. Variation of the amplitude spectra of focused waves at different locations with current U_0 = 0.0 m/s.

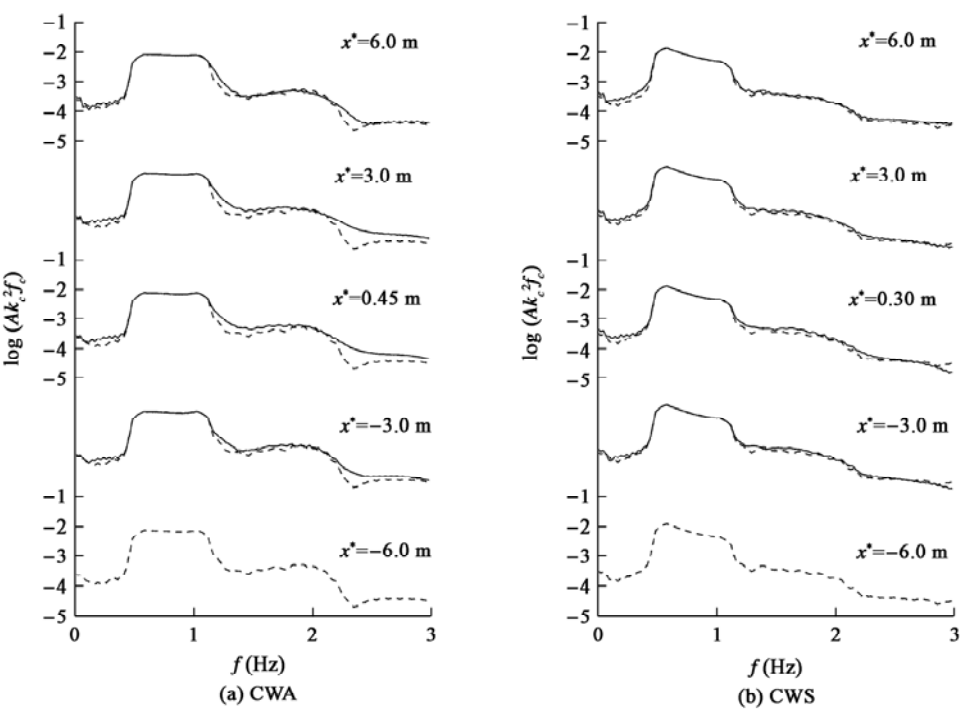

Fig. 8. Variation of amplitude spectra of focused waves at different locations with current U_0 = 0.1 m/s.

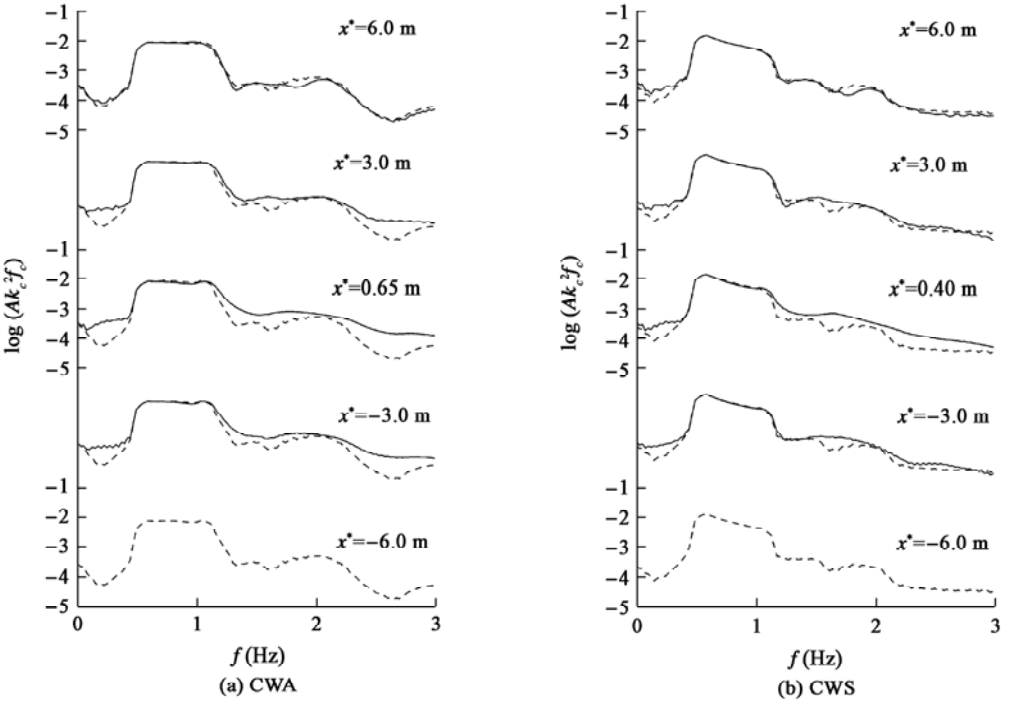

Fig. 9. Variation of amplitude spectra of focused waves at different locations with current $U_0 = -0.1$ m/s.

4. Conclusions

In the present study, a numerical model based on the HOS method is successfully developed to simulate the wave focusing on current. The influence of current on wave focusing is numerically investigated. The calculated results show that the current has significant influence on wave focusing. The wave crest becomes steeper and the energy transform becomes bigger for waves with opposing current. It reveals that there is strong nonlinear interaction for the wave transformation on opposing current. It means that the freak wave occurs more likely when wave propagates with opposing current. In addition, the frequency spectrum which represents the wave component distribution can also affect the interaction between the focused wave and current. The focused wave with CWA spectrum can obtain bigger maximum crest and more significant energy transfer than that with CWS spectrum.

References

Baldock, T. E. and Swan, C., 1996. Extreme waves in shallow and intermediate water depths, *Coast. Eng.*, **27**(1-2): 21~46.

Bonnefoy, F., Touzé, D. and Ferrant, P., 2004. Generation of fully-nonlinear prescribed wave fields using a high-order spectral model, *Proc. 14th Int. Offshore Polar Eng. Conf.*, Toulon, France, 23~28.

Dommermuth, D. G. and Yue, D. K. P., 1987. A high-order spectral method for the study of nonlinear gravity waves, *J. Fluid Mech.*, **184**, 267~288.

Fochesato, C., Grilli, S. and Dias, F., 2007. Numerical modeling of extreme rogue waves generated by directional energy focusing, *Wave Motion*, **44**(5): 395~416.

Gibson, R. S. and Swan, C., 2007. The evolution of large ocean waves: the role of local and rapid spectral changes, *Proc. R. Soc. Lond.*, *Ser. A*, **463**(2077): 21~48.

Johannessen, T. B. and Swan, C., 2003. On the nonlinear dynamics of wave groups produced by the focusing of surface water waves, *Proc. R. Soc. Lond.*, *Ser. A*, **459**(2032): 1021~1052.

Kharif, C. and Pelinovsky, E., 2003. Physical mechanisms of the rogue wave phenomenon, *Eur. J. Mech. B*/*Fluids*, **22**(6): 603~634.

Lavrenov, I. V. and Porubov, A. V., 2006. Three reasons for wave generation in the non-uniform current, *Eur. J. Mech. B*/*Fluids*, **25**(5): 574~585.

Li, J., Liu, S. and Hong, K., 2008. Numerical study of two-dimensional focusing waves characteristics, *China Ocean Eng*., **22**(2): 253~266.

Liu, S. and Hong, K., 2005. Physical investigation of directional wave focusing and breaking waves in wave basin, *China Ocean Eng*., **19**(1): 21~35.

Liu, S., Li, J. and Sun, Y., 2008. Numerical investigation of multidirectional wave focusing properties, *Proc. 18th Int. Offshore Polar Eng. Conf.*, Vancouver, Canada, 6~11.

Lynett, P., 2002. *A Multi-Layer Approach to Modeling Generation, Propagation, and Interaction of Water Waves*, Ph.D. Thesis, Cornell University.

Nepf, H. M., Wu, C. H. and Chan, E. S., 1998. A comparison of two- and three-dimensional wave breaking, *J. Geophys. Res.*, **28**(7): 1496~1510.

Rapp, R. J. and Melville, W. K., 1990. Laboratory study of steep and breaking waves, *Phil. Trans. R. Soc. Lond.*, **A331**, 735~780.

Wu, C. H. and Yao, A., 2004. Laboratory measurements of limiting freak waves on current, *J. Geophys. Res.*, **109**, C12002, dio:10.1029/2004JC002612.

Touboul, J., Pelinovsky, E. and Kharif, C., 2007. Nonlinear focusing wave group on current, *Journal of Korean Society of Coastal and Ocean Engineering*, **19**(3): 222~227.

Zakharov, V. E., 1968. Stability of periodic waves of finite amplitude on the surface of a deep fluid, *Journal of Applied Mechanics and Technical Physics*, **9**(2): 190~194. (English transl)